implies that if there are no conjugate (focal) points relative to a fixed (variable) endpoint A, and the appropriate matrix evaluated at the opposite endpoint B is positive definite, then there are also no conjugate (focal) points relative to fixed (variable) endpoint B, and the appropriate matrix evaluated at A is positive definite. A third equivalent set of conditions involves forward integration of the Riccati equation from the initial point to some intermediate point and backward integration of the Riccati equation from the terminal point to the same intermediate point. The difference between these matrices is required to be positive-definite at this point, for sufficiency.

These sets of sufficient conditions are minimal sets. Weakened versions of these conditions are found to be necessary for a weak minimum. The necessary conditions involving a backward or forward sweep are found to be equivalent to the second-order condition of Brusch and Vincent[5] plus a modified conjugate point condition. The sweep conditions are applicable to a broader class of problems and appear to be significantly easier to implement, in most cases. Both the sweep conditions and Brusch and Vincent's condition are far easier to apply than the classical conditions of Bliss.[1,11]

The forward, backward, and forward-backward sweeps discussed in this paper are also useful in smoothing and following problems for linear systems.[12]

References

[1]Bliss, G. A., *Lectures on the Calculus of Variations*, University of Chicago Press, Chicago, Ill., 1946, pp. 187–265.

[2]McReynolds, S. R., "A Successive Sweep Method for Solving Optimal Programming Problems," Ph.D. thesis, 1965, Dept. of Applied Mathematics, Harvard University, Cambridge, Mass.

[3]Bryson, A. E., Jr. and Ho, Y. C., *Applied Optimal Control*, Blaisdell, Waltham, Mass., 1969, pp. 42–89, 177–211.

[4]Schmitendorf, W. E. and Citron, S. J., "On the Applicability of the Sweep Method to Optimal Control Problems," *IEEE Transactions on Automatic Control*, Vol. AC-14, No. 1, Feb. 1969, pp. 69–72.

[5]Brusch, R. G. and Vincent, T. L., "Numerical Implementation of a Second-Order Variational Endpoint Condition," *AIAA Journal*, Vol. 8, No. 12, Dec. 1970, pp. 2230–2235.

[6]Vincent, T. L. and Brusch, R. G., "Optimal Endpoints," *Journal of Optimization Theory and Applications*, Vol. 6, No. 4, Oct. 1970, pp. 299–319.

[7]Wood, L. J. and Bryson, A. E., Jr., "Second-Order Optimality Conditions for Variable End Time Terminal Control Problems," *AIAA Journal*, Vol. 11, No. 9, Sept. 1973, pp. 1241–1246.

[8]Wood, L. J., "Second Order Optimality Conditions and Optimal Feedback for Variable End Time Terminal Control Problems," Ph.D. dissertation, 1972, Dept. of Aeronautics and Astronautics, Stanford University, Stanford, Calif.

[9]Dreyfus, S. E., *Dynamic Programming and the Calculus of Variations*, Academic Press, New York, 1965, pp. 156–157.

[10]Wood, L. J., "Perturbation Guidance for Minimum Time Flight Paths of Spacecraft," AIAA Paper 72-915, Palo Alto, Calif., 1972.

[11]Bliss, G. A., "The Problem of Bolza in the Calculus of Variations," *Annals of Mathematics*, Vol. 33, 1932, pp. 261–274.

[12]Bryson, A. E., Jr. and Hall, W. E., Jr., "Optimal Control and Filter Synthesis by Eigenvector Decomposition," Rept. 436, 1971, Stanford University, Dept. of Aeronautics and Astronautics, Stanford, Calif.

APRIL 1974 J. AIRCRAFT VOL. 11, NO. 4

Study of Wind Effects on Electrostatic Autopilots

Edmund Sullivan Jr.*
Naval Underwater Systems Center, Newport, R.I.

The electrostatic autopilot is a device which uses the Earth's vertical potential gradient as a roll and pitch reference by measuring the potential difference between wing tips and between nose and tail. Small radioactive sources are used to ionize the air at the points between which the measurements are made. This serves to supply charge for a differential amplifier. Wind-tunnel tests on this device have shown that the output is wind-speed dependent. The output is virtually zero for zero wind speed and increases to a stable value at about 25 m/sec. A simplified mathematical model is presented as an explanation of this behavior. The model suggests that, as the wind speed increases, the ionized air is drawn into long streams thus reducing the charge density. This in turn reduces losses due to recombination which results in a greater total charge available. Results of calculations based upon this model are in qualitative agreement with experiment.

Nomenclature

A = area
a = length of wire
E_o = unperturbed electric field intensity
e = charge of the electron
I = current
k_1, k_2 = positive and negative ion mobilities
L = length of side of cubic ionized region
q = rate of creation of ionized pairs per unit volume
V = wind speed
α = recombination coefficient
β = charge removal coefficient
ρ = ionized pair density
ρ_o = ionized pair density for zero wind speed

Received December 6, 1973; revision received February 26, 1974.
Index category: Aircraft Handling, Stability, and Control.
*Physicist, Weapons Department.

I. Introduction

RECENT work by Hill[1] utilizing the earth's vertical potential gradient as a reference for aircraft control has resulted in a remarkably simple and workable system. Thunderstorm activity in the atmosphere serves to transfer negative charge to the earth which results in a potential difference between earth and ionosphere of approximately 10^5 v.[2] The potential gradient varies from about 160 v/m at the earth's surface to values of the order of 5 v/m at an altitude of 20 km. As shown by Hill,[1] one can

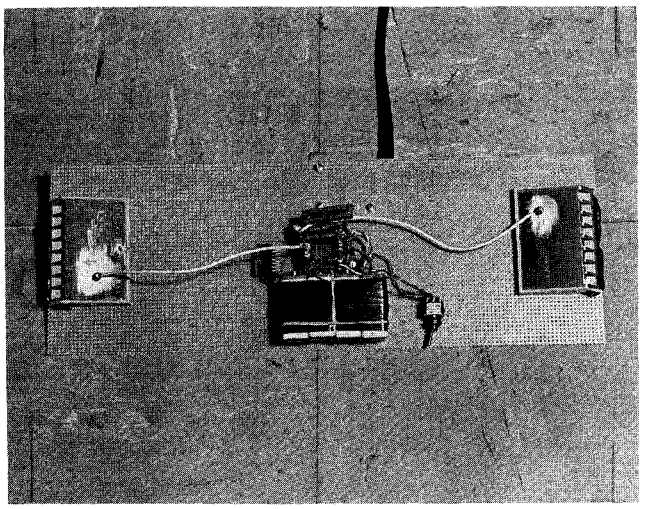

Fig. 1 View of experimental sensor. The radioactive sources are situated on each end and the amplifier and battery pack are in the center. The mounting board is approximately 13 in. long.

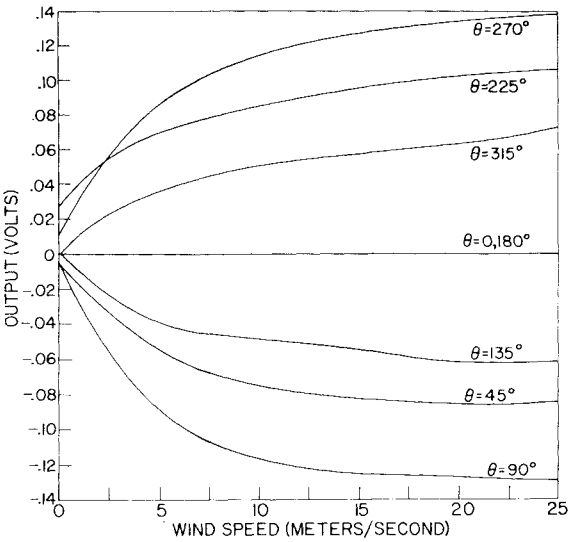

Fig. 3 Output voltage vs wind speed. θ is the angular position of the sensor in the wind tunnel with respect to the horizontal.

utilize this potential gradient as an autopilot reference by simply measuring the potential difference between wing tips and between nose and tail to indicate roll and pitch angle, respectively. Small radioactive sources are used to ionize the air in the two regions between which the measurement is made. The ionized air then serves as a source of charge for a differential amplifier. A thorough discussion of the atmosphere physics involved along with a discussion of several models utilizing such autopilots is given in Ref. 1.

Wind-tunnel tests of such a system carried out at the Naval Underwater Systems Center manifested a phenomenon which, at the time, was quite mystifying. The output of the system was extremely noisy and bore no correlation to the angular position of the device with respect to the electric field. As the wind speed was increased from zero, however, the noise diminished and the output increased to the point where the system became quite workable. Following a report on the experimental wind-tunnel work, a mathematical model is presented which yields qualitative agreement with the experimental results.

II. Background

The device used in the wind-tunnel tests is shown in Fig. 1. The amplifier in the center is a Burr-Brown 3621K which has an input impedance of 10^{11} Ω in the differential mode. The radioactive sources are placed 13 in. apart and are separated by 400 MΩ of resistance across which the differential amplifier is connected. These sources are the cartridges from "staticmaster 500" electrostatic brushes. Each source contains 500 microcuries (μc) of polonium 210 ($_{84}Po^{210}$). This is equivalent to 0.025 micrograms (μg). The half life of $_{84}Po^{210}$ is 138 days and the decay product is chiefly alpha particles.

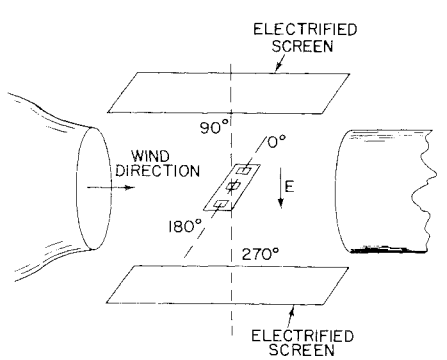

Fig. 2 Schematic view of wind-tunnel arrangement.

The device was placed in the wind tunnel as shown schematically in Fig. 2. The two electrified screens, which were about 5 ft square and 5 ft apart, produced an electric field intensity of 115 v/m.

Figure 2 depicts the unit at 0°. That is, there should be zero voltage between the two radioactive sources in this position since the electric field vector is vertical. Measurements were taken at intervals of 45°. The results of these measurements are shown in Fig. 3. It is to be noted here that, up to about 25 m/sec, the output is strongly wind-dependent. This behavior was rather unexpected and led to the theory proposed in Sec. III. Along with this wind-dependent behavior was the fact that at low velocities the output was quite noisy. This noise diminished as the wind speed approached 25 m/sec. This would be expected since the slopes of the curves in Fig. 3 would require that wind-speed fluctuations be reflected in the output in a manner proportional to the magnitude of these slopes.

III. Discussion

For purposes of analysis, the following simplified system is adopted: The two radioactive sources are assumed to be connected by a zero resistance wire which is parallel to the electric field vector. The electric field now has the configuration shown by the field mapping in Fig. 4. Figure 4 is a two-dimensional field mapping whereas the problem being dealt with here is three-dimensional. The two-dimensional solution is used since it considerably simplifies things, and in the qualitative spirit of this treatment, should not produce an intolerable error. Further assumptions adopted are the following:

1) The ionized region around each ionization source, when the wind is "off," is a cube of side L where $L = \tau^{1/3}$. τ is the volume of a hemisphere of radius 3.8 cm^3. This is the range of an alpha particle ejected by $_{84}Po^{210}$.

2) When the wind is "on," two plasma streams are blown in the X direction in "tubes" of square cross section having area L^2.

3) The electric field at the plasma streams is assumed normal to the plasma streams and has the value E_o for all values of X.

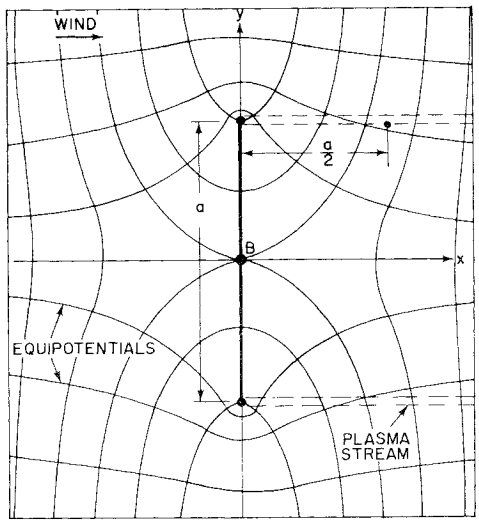

Fig. 4 Idealized electric field map. Point B is the center of the sensor. The plasma streams represent the ionized air being blown away from the radioactive sources by the wind.

4) The plasma streams do not perturb the electric field pattern.

5) The cubic ionized regions at the sources, located between $X = 0$ and $X = -L$, contain an ionized pair density, ρ_o, which is not dependent upon X.

Consider now the situation when the wind is turned on. Charge will be drawn from the plasma tubes and be carried along the field lines. Since the field lines which originate between $X = 0$ and $X \cong a/2$ terminate on the wire, the total current carried on these field lines must pass through the point B (see Fig. 4). The problem then, is to calculate this current at B as a function of the wind speed V. In order to accomplish this, it is first necessary to calculate the density of ionized pairs in the plasma streams as a function of X. Letting this density be presented by ρ, a generalized continuity equation can now be written as

$$\nabla \cdot (\rho \vec{V}) + \frac{\partial \rho}{\partial t} - q + \beta\rho + \alpha\rho^2 = 0 \tag{1}$$

The term $\beta\rho$ accounts for the removal of charge by the electric field. An expression for β will be derived later. The $\alpha\rho^2$ term accounts for charge lost through recombination of positive ions and electrons. α is referred to as the coefficient of recombination and, as will be seen later, is a very crucial parameter in this problem. Finally, q represents the rate of creation of ionized pairs per unit volume. This term is zero everywhere except in the region $-L < X < 0$. In the region for all $X > 0$, at time equilibrium, Eq. (1) becomes

$$V\frac{d\rho}{dx} + \beta\rho + \alpha\rho^2 = 0 \tag{2}$$

Here, the wind velocity has been picked to be in the X direction. Equation (2) can be immediately integrated. Upon integration and solving for ρ one finds that

$$\rho = \frac{\beta\rho_o \exp(-\beta x/V)}{\alpha\rho_o + \beta - \alpha\rho_o \exp(-\beta x/V)} \tag{3}$$

In order to determine ρ_o, $d\rho/dX$ is assumed to be zero for $-L < X < 0$ (assumption 5) so that at equilibrium Eq. (2) becomes

$$\alpha\rho_o^2 + (V/L)\rho_o - q = 0 \tag{4}$$

The term $V\rho_o/L$ has been added to account for the loss of ionized pairs through the face of the cube normal to the X axis. Equation (4) has the solution

$$\rho_o = -(V/2\alpha L) + \left[(V/2\alpha L)^2 + \frac{q}{\alpha}\right]^{1/2} \tag{5}$$

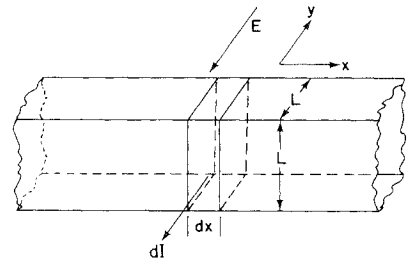

Fig. 5 Differential volume LdX from Eq. (7).

Before calculating the current, a final task is to determine β. The current in a plasma due to an electric field is given by

$$I = Ae\rho(k_1 + k_2)E_o \tag{6}$$

For a differential unit of area LdX (see Fig. 5), Eq. (6) becomes

$$dI = Le\rho(k_1 + k_2)E_o dx \tag{7}$$

Now, since the term $\beta\rho$ is the rate of change of ionized pair density due to the electric field, it follows that

$$dI = 2\beta\rho L^2 e dx \tag{8}$$

The factor of 2 is to account for the fact that ρ is an ionized *pair* density and not a charge density. Combining Eqs. (7) and (8), results in

$$\beta = (k_1 + k_2)E_o/(2L) \tag{9}$$

The total current at the point B can now be calculated. Eliminating ρ from Eq. (8) with Eq. (3) leads to the following integral:

$$I = \frac{2L^2 e\beta^2}{\alpha}\int_0^{a/2} \frac{\exp(-\beta x/V)}{K - \exp(-\beta x/V)}\, dx \tag{10}$$

Here,

$$K = \frac{\alpha\rho_o + \beta}{\alpha\rho_o}$$

Integration yields

$$I = \frac{2L^2 e\beta V}{\alpha} \ln\left\{\frac{K - \exp[-\beta a/(2V)]}{K - 1}\right\} \tag{11}$$

The values of the various parameters contained in Eq. (11) are: $L = 0.0486$ m, $E_o = 115$ v/m, $a = 0.33$ meters, $k_1 = 1.29 \times 10^{-4}$ m^2/v/sec, $k_2 = 1.82 \times 10^{-4}$ m^2/v/sec, and $e = 1.6 \times 10^{-19}$ coulomb. The two remaining parameters are q and α. The ionization sources each contain 0.025 μg of $_{84}Po^{210}$. This information plus the half life of $_{84}Po^{210}$, the mass of a nucleon, the alpha particle range, and the number of ionized pairs per unit length created by the alpha particle[3] allow one to determine that

$$q = 9.5 \times 10^{14} \text{ ionized pairs/m}^3\text{/sec} \tag{12}$$

This calculation assumes that the Polonium is "fresh."

The value of α has had a rather interesting history. Some of the earlier measurements were shown to be in error due to the fact that its value, among other things, depends upon how the ionization is produced during the

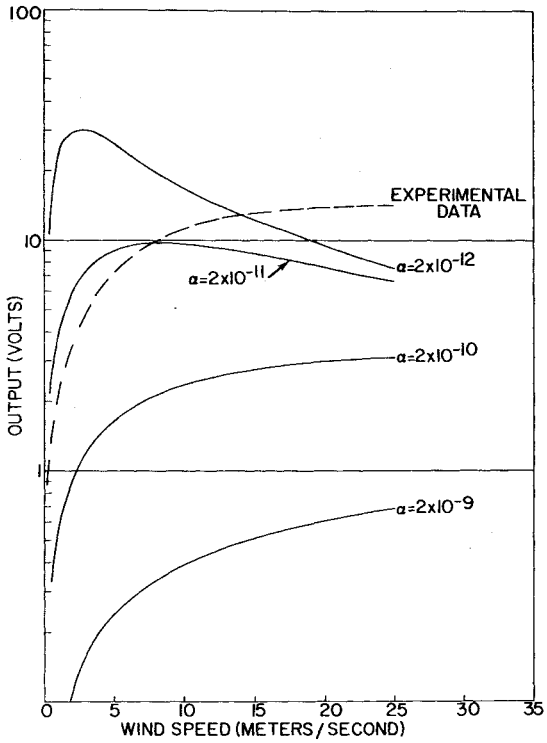

Fig. 6 Comparison of theory to experimental results. The dotted curve represents the experimental case for $\theta = 90°$. Unlike Fig. 3, the voltage scale here reflects the factor of 100 due to the amplifier.

measurement. In particular, if the ionization is due to alpha radiation, as it is here, α turns out to be time-dependent.[4] This is due to the fact that the alpha particle tracks generate regions of high ionization density in the neighborhood of the tracks with regions of low ionization density between the tracks.[4] This results in an initial high value of α which decreases in time as these tracks of high ionization density diffuse. For times up to about 0.5 sec, α can vary as much as a few orders of magnitude. To include this phenomenon in this calculation would produce tremendous difficulties. Instead, the point of view is taken that there is some effective constant value for α which is determined by treating it as a parameter of variation. The value of α for large values of time is of the order of 2.0×10^{-12} m^3/sec for air at STP.

IV. Results

Although the current at point B has been calculated, we prefer to know the voltage dropped across the 400 MΩ resistance in order to compare the calculation directly with experiment. Multiplying the current by 4×10^8 Ω results in a fraction of a volt. The voltage between the plasma streams, on the other hand, is several volts except for regions very near the wire. Hence, the 400 MΩ resistance has negligible effect, and simply multiplying Eq. (11) by 4×10^8 Ω to obtain the voltage is justified.

Figure 6 shows the voltage observed in the wind tunnel tests as a function of wind speed for the case $\theta = 90°$. Along with this curve are plotted the results of this calculation for several values of α. The voltage values in Fig. 6 reflect the gain of the amplifier. This gain was arbitrarily set to 100.

It is seen that the curve for $\alpha = 2.0 \times 10^{-10}$ m^3/sec is within about a factor of four of the experimental data and has approximately the same shape.

Bearing in mind the crudeness of the model, these results could be considered reasonably close. Of course, where one has a free parameter, "closeness" of fit is not too meaningful. However, since the curves do have roughly the same shape as the experimental curve, it is felt that the model does demonstrate the mechanism involved here.

Since only the region of the plasma stream between $X = 0$ and $X = a/2$ actually contributes to the current, ultimately the current must decrease for large enough wind speed. As can be seen from Fig. 6, this does occur in the model for α smaller than 2.0×10^{-10}. Since it was not possible to attain wind speeds greater than 25 m/sec in the wind tunnel, this phenomenon was not actually observed experimentally.

V. Conclusions

In summary, the sensitivity of the electrostatic autopilot is wind speed dependent. The importance of this behavior, however, appears to depend upon the value of a parameter (α) which is not well known. As noted in Sec. IV, the current decreases for large enough wind speeds. It can be shown by means of Eq. (11) that as V approaches infinity, I approaches zero. Figure 6 indicates the sensitivity of this behavior to α. It would appear that if the true value of α turned out to be small enough, the speed of the aircraft would be an important factor to consider in high-speed applications of electrostatic autopilots.

From a more heuristic point of view, this phenomenon can be understood in terms of the ionized pair density ρ. As the wind speed increases, the density of ionized pairs decreases due to the charge being drawn out in long streams. This, in turn, must decrease the recombination rate. The result is more total charge and, therefore, more current as long as enough of the ions are still within the limits of integration. After this condition is no longer fulfilled, the amount of total charge contributing to the current begins to decrease as observed.

References

[1]Hill, M. L., "Introducing the Electrostatic Autopilot," *Astronautics and Aeronautics*, Vol. 10, No. 11, Nov. 1972, pp. 22-31.

[2]Fleagle, R. G. and Businger, J. A., *An Introduction to Atmospheric Physics*, Academic Press, New York, 1963, Chap. 3.

[3]Etherington, H., ed., *Nuclear Engineering Handbook*, McGraw-Hill, New York, 1958, pp. 7-34.

[4]Loeb, L., *Basic Processes of Gaseous Electronics*, University of California Press, Berkeley and Los Angeles, 1960, Chap. 6.